

Adiabatically tapered periodic segmentation of channel waveguides for mode-size transformation and fundamental mode excitation

M. H. Chou, M. A. Arbore, and M. M. Fejer

E. L. Ginzton Laboratory, Stanford University, Stanford, California 94305

Received November 27, 1995

We report modeling, fabrication, and characterization of tapered waveguides, using periodically segmented annealed proton exchange in LiNbO₃. For a taper transforming the $1/e$ full width (intensity) mode size from $6.0 \mu\text{m} \times 4.4 \mu\text{m}$ to $2.0 \mu\text{m} \times 1.3 \mu\text{m}$, 0.4-dB excess loss was observed. The large, slightly elliptical mode can ease coupling to single-mode fibers and circular free-space beams. The same taper structure was used to excite a highly multimoded (13 modes) waveguide with more than 95% of the power stably launched into the lowest-order mode. This function is useful for nonlinear waveguide devices, such as difference-frequency generators, in which modes at highly disparate wavelengths interact. © 1996 Optical Society of America

Transformation of modal properties through axial tapering of a dielectric waveguide is useful in several contexts. Mode-size transformation permits independent optimization of the mode size in different portions of a waveguide for effective input and output coupling and for efficient performance of active or electro-optic devices. An adiabatic taper from a single-mode to a multimode waveguide also permits robust coupling into the fundamental mode of a multimode waveguide, important in certain types of nonlinear waveguide devices that involve interactions between modes at widely disparate wavelengths. Although several techniques are available for growth of axially varying III–V semiconductor waveguides,^{1,2} less progress has been made for tapers in diffused waveguides in insulating crystals. Periodically segmented waveguides^{3–9} (PSW's) permit independent control over vertical and lateral confinement and thus can be used to tailor the size and shape of waveguide modes. In this Letter we report on modeling, fabrication, and characterization of tapers in annealed proton-exchanged waveguides in LiNbO₃ through the use of segmentation with an axially varying duty cycle, with emphasis on applications in nonlinear waveguide devices.

In a difference-frequency mixer, a pump at frequency ω_p mixes with a signal at frequency ω_s to generate an idler at frequency $\omega_i = \omega_p - \omega_s$. This interaction is useful both for generating mid-infrared radiation from near-infrared pumps^{10–12} and for wavelength conversion in wavelength-division-multiplexed communication systems.^{13,14} One or both of signal and idler must be at significantly longer wavelengths than the pump, so a waveguide that supports modes at the longest wavelength is necessarily multimoded at the pump wavelength. It is difficult to couple pump radiation robustly into the fundamental mode of such a multimoded structure, a problem that has precluded practical application of the large mixing efficiencies that have been demonstrated in such devices.^{10,12}

For applications with two short-wavelength inputs this mode-coupling problem can be solved with a tapered waveguide structure. The two inputs are coupled into a waveguide that is single moded at both

input wavelengths but cut off at the output wavelength. A subsequent adiabatic taper into a waveguide that guides the output wavelength permits efficient coupling of the input radiation into the fundamental modes of the highly multimoded waveguide in which the nonlinear mixing takes place.

Whereas it is straightforward to taper the lateral dimension of a waveguide by lithographic means, tapering the vertical dimension requires techniques that are difficult to control, such as diffusion in a temperature gradient and deposition of a nonuniform film. Because it is necessary to taper both dimensions to accomplish either a significant mode size or ellipticity transformation, a technique that permits control of the vertical confinement is required.

Periodically segmented waveguides, consisting of segments of length l indiffused with a dopant to produce an index change Δn , separated by undoped regions with a repeat period Λ , permit flexibility in tailoring waveguide properties. It has been shown theoretically that an average index model, in which the behavior of the PSW is approximated by an equivalent waveguide in which the refractive-index step is

$$\Delta n_{\text{eq}} = \Gamma \Delta n, \quad (1)$$

with a duty cycle $\Gamma = l/\Lambda$, accurately predicts the modal properties of the waveguide.⁴ Experimental verification of the accuracy of the model of Eq. (1) has been obtained for annealed-proton-exchanged waveguides.⁶ Nir *et al.* showed that under appropriate fabrication conditions the propagation losses are not significantly increased over a similarly confining uniform waveguide.⁹ With independently controllable optical confinement in both width (with physical width and segmentation duty cycle) and depth (with segmentation duty cycle), the segmented waveguide with axially varying duty cycle shown in Fig. 1 is a practical method to make tapered waveguides.

We designed PSW tapers, using beam-propagation method¹⁵ (BPM) simulations, with either the average index model of Eq. (1) or a model explicitly treating the periodic (abrupt) index variations. In both

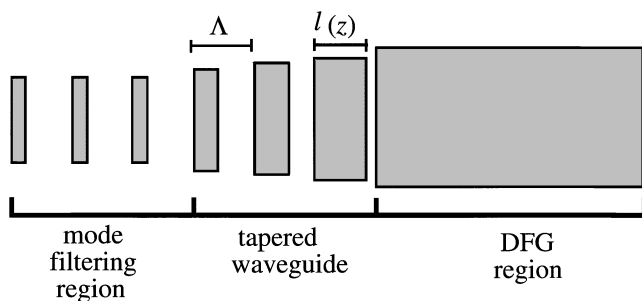


Fig. 1. Schematic of an adiabatic taper using a periodically segmented structure integrated with a multimoded waveguide designed for difference-frequency generation (DFG).

cases we used the effective index approximation and used the two-dimensional BPM separately in depth and width. Predictions from these two models should bound the actual properties of diffused tapers because they assume continuous or maximally discontinuous refractive-index distributions, whereas real tapers exhibit axially diffused (smoothed) distributions. Two quantities characterize the taper: the throughput, defined as the ratio of the power coupled out to that coupled in, and the mode-excitation efficiency, defined as the ratio of the power output in the fundamental mode to the total output power. For the tapers considered here we found that the mode-excitation efficiency predictions based on the average index model agreed well with those of the periodic model, whereas the throughput predictions agreed only qualitatively.

We chose for a demonstration a taper that couples pump radiation (780 nm) into the fundamental mode of a waveguide designed for near-degenerate difference-frequency mixing at $1.56 \mu\text{m}$, thus constraining the waveguide (and taper) fabrication conditions. Using the annealed-proton-exchanged LiNbO_3 waveguide model of Ref. 16, we chose a proton-exchange depth and width of 0.5 and $5.5 \mu\text{m}$, respectively, and an annealing time of 9 h at 333°C , giving a nominally 13-moded waveguide for the pump. Our modeling indicated that a 0.1–1-mm-long input coupling region segmented with a period of $10 \mu\text{m}$ and a duty cycle of 0.2 is single moded at 780 nm and effective as a mode filter. We fixed the length at 1 mm and the width at $5 \mu\text{m}$ and evaluated several functional forms of tapered duty cycle: convex with $\Gamma(z) = 0.2 + 0.8z^{1/2}$, linear with $\Gamma(z) = 0.2 + 0.8z$, and concave with $\Gamma(z) = 0.2 + 0.8z^3$, where z (in millimeters) is the axial coordinate. These simulations predicted throughput greater than 96% for all three tapers and mode excitation efficiencies of 78%, 92%, and 98% for the convex, linear, and concave tapers, respectively.

Samples with these designs for 780-nm operation were fabricated by proton exchange through a SiO_2 mask in pure benzoic acid for 2.5 h at 177°C and annealing in air at 333°C for 9 h. The samples were then tested for spatial mode profiles, dependence of output mode on input coupling conditions, taper losses, and mode-excitation efficiency. The measured $1/e$ intensity dimensions of the fundamental mode were $6.0 \mu\text{m} \times 4.4 \mu\text{m}$ in the single-mode (segmented)

sections and $2.0 \mu\text{m} \times 1.3 \mu\text{m}$ in the multimode (homogeneous) sections, in reasonable agreement with the theoretical values of $5.8 \mu\text{m} \times 3.5 \mu\text{m}$ and $1.9 \mu\text{m} \times 1.3 \mu\text{m}$, respectively. To measure the product of mode-excitation efficiency and throughput in the taper (excess loss), we fabricated 11-mm-long straight segmented waveguides with and without back-to-back tapers. Both of these waveguides are single mode at their input and output ends and therefore could be tested by the Fabry–Perot method.¹⁷ The total propagation loss of the straight-segmented guide was 1.1 dB (1.0 dB/cm). The total loss for the segmented waveguide with two 1-mm-long concave tapers was 2.3 dB. Subtracting the losses of the straight sections leaves an excess loss of 0.6 dB for each of the 1-mm concave tapers. Similarly, we obtain excess losses of 1.5 dB for 1-mm linear tapers and 0.4 dB for 2.5-mm-long concave tapers. Although these trends are consistent with predictions, our BPM simulations predict approximately a factor of 1.5–2 lower losses. The source of this discrepancy is not clear.

We used modal interference to measure the mode-excitation efficiency. When more than one mode is excited in the waveguide, the output intensity distribution is determined by the coherent sum of the modal fields present at the output of the waveguide. To quantify the fraction of power in the fundamental mode, we observed the output intensity distribution while tuning the excitation laser. Wavelength dependence of the output intensity distribution results from

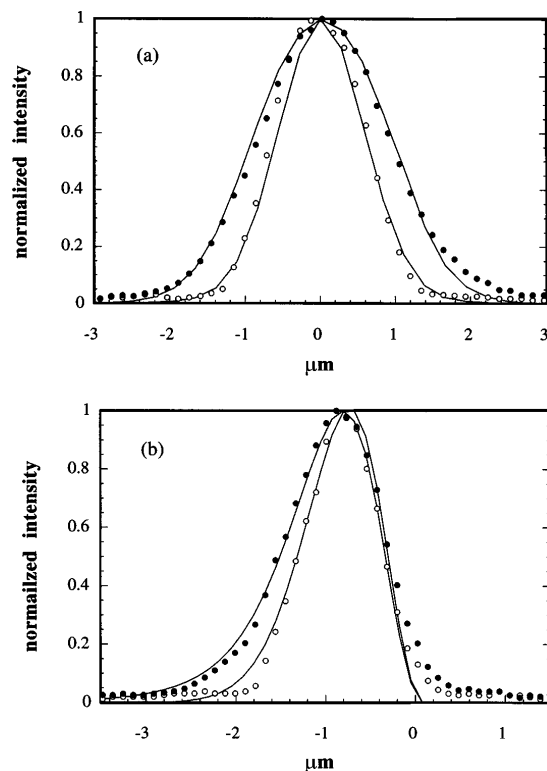


Fig. 2. Output intensity profiles showing modal interference. Open and filled circles were measured at two wavelengths near 780 nm; solid curves are fits for 0 and π relative phases between the fundamental and the first allowed high-order transverse modes (a) in the width direction and (b) in the depth direction.

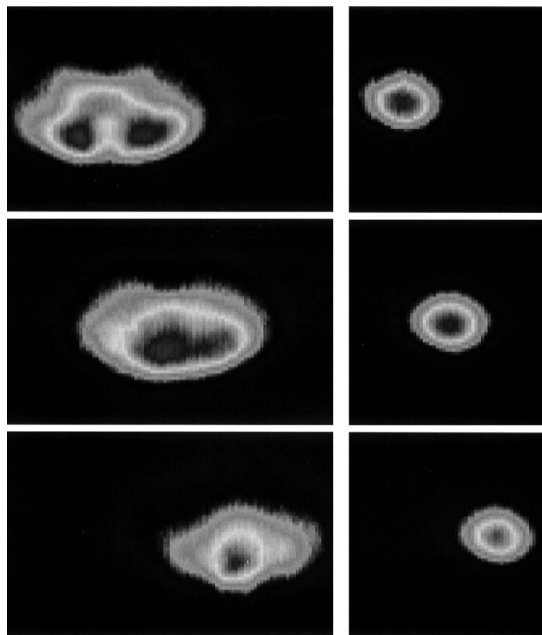


Fig. 3. Measured output intensity profiles for different input coupling conditions for launching the light into a waveguide without any taper (left) and with a concave taper (right). In this example, waveguides are moved in the width direction $\sim 1.7 \mu\text{m}$ relative to the incident beam to change coupling conditions. Output is stably in the fundamental mode after launching through the taper, unlike when it is launched directly into the waveguide.

modal dispersion between the fundamental and higher-order modes, which then add in or out of phase with each other as the wavelength is varied. Assuming (as predicted by simulations) that the second-higher-order width mode and the first-higher-order depth mode dominate the undesired modal excitation, the observed output can be fitted with respect to the ratio of fundamental mode to higher-order mode power. Figure 2 shows the measured output intensity profiles of maximum and minimum widths in a multimode guide, in which light has been launched through a 1-mm concave taper. The solid curves are fits for 0 and π relative phases of the fundamental and higher-order modes, corresponding to mode excitation efficiencies of 97% in width and 98% in depth, resulting in 95% overall. These figures are again in reasonable agreement with the 98% overall efficiency predicted from simulations. Qualitative mode imaging verified the better mode-excitation performance predicted by BPM for the concave taper compared with the linear and convex tapers.

We tested the sensitivity of the output intensity distribution to the input coupling conditions to illustrate that the filtering of the input coupling region prevents launching of undesired modes. Figure 3 shows measured output intensity distributions observed with different input coupling conditions for two waveguides differing only in that one had a 1-mm-long concave input taper and the other did not. The waveguides were moved laterally (shown) and vertically $\sim 1.7 \mu\text{m}$. It

can be seen that the output mode mixture for the waveguide with no taper is highly sensitive to input coupling conditions, whereas the mode mixture for the waveguide with the coupling taper is not.

In summary, we have used a segmented structure to fabricate tapered annealed proton-exchanged channel waveguides in LiNbO_3 . The results are in good agreement with an average index model for the segmented waveguides. Spot-size transformations of 3:1 have been obtained, with excess losses of 0.4 dB. The large dimensions of the single guided mode at the input simplify coupling and increase stability for free-space launching and also should prove useful for efficient fiber pigtailling. The output mode of the taper is the fundamental transverse mode of the multimoded waveguide, regardless of the alignment of the input beam. Additionally, PSW tapers can be integrated with essentially any existing integrated-optic device without requiring additional lithography or diffusion steps.

This research is supported by the Advanced Research Projects Agency through the Center for Nonlinear Optical Materials and the Optoelectronics Materials Center and by the Joint Services Electronics Program. We also acknowledge the generosity of Crystal Technology and New Focus for materials and equipment.

References

1. A. Shahar, W. J. Tomlinson, A. Yi-Yan, M. Seto, and R. J. Deri, *Phys. Lett.* **56**, 1098 (1990).
2. H. S. Kim, S. Sinha, and R. V. Ramaswamy, *IEEE Photon. Technol. Lett.* **5**, 1049 (1993).
3. Z. Weissman and A. Hardy, *Electron. Lett.* **28**, 1514 (1992).
4. Z. Weissman and A. Hardy, *J. Lightwave Technol.* **11**, 1831 (1993).
5. Z. Weissman and I. Hendel, *J. Lightwave Technol.* **13**, 2053 (1995).
6. F. Dorgeuille, B. Mersali, S. Francois, G. Hervé-Gruyer, and M. Filoche, *Opt. Lett.* **20**, 581 (1995).
7. L. Li and J. J. Burke, *Opt. Lett.* **17**, 1195 (1993).
8. K. Thyagarajan, C. W. Chein, R. V. Ramaswamy, H. S. Kim, and H. C. Cheng, *Opt. Lett.* **19**, 880 (1994).
9. D. Nir, S. Ruschin, A. Hardy, and D. Brooks, *Electron. Lett.* **31**, 186 (1995).
10. H. Herrmann and W. Sohler, *J. Opt. Soc. Am. B* **5**, 278 (1988).
11. E. J. Lim, H. M. Hertz, M. L. Bortz, and M. M. Fejer, *Appl. Phys. Lett.* **59**, 2207 (1991).
12. S. Sanders, D. W. Nam, R. J. Lang, M. L. Bortz, and M. M. Fejer, in *Conference on Lasers and Electro-Optics*, Vol. 8 of 1994 OSA Technical Digest Series (Optical Society of America, Washington, D.C., 1994), p. 287.
13. C. Xu, H. Okayama, K. Shinozaki, K. Watanabe, and M. Kawahara, *Appl. Phys. Lett.* **63**, 1170 (1993).
14. M. L. Bortz, D. Serkland, M. M. Fejer, and S. J. B. Yoo, in *Conference on Lasers and Electro-Optics*, Vol. 8 of 1994 OSA Technical Digest Series (Optical Society of America, Washington, D.C., 1994), p. 288.
15. M. D. Feit and J. A. Fleck, Jr., *Appl. Opt.* **20**, 848 (1981).
16. M. L. Bortz and M. M. Fejer, *Opt. Lett.* **16**, 1844 (1991).
17. R. Regener and W. Sohler, *Appl. Phys. B* **36**, 143 (1985).